

Cardiovascular, Pulmonary and Renal Pathology

Activin-Like Kinase 5 (ALK5) Mediates Abnormal Proliferation of Vascular Smooth Muscle Cells from Patients with Familial Pulmonary Arterial Hypertension and Is Involved in the Progression of Experimental Pulmonary Arterial Hypertension Induced by Monocrotaline

Matthew Thomas,* Cerys Docx,* Alan M. Holmes,* Sarah Beach,* Nicholas Duggan,* Karen England,* Catherine Leblanc,[†] Clemence Lebret,* Francis Schindler,* Farheen Raza,* Christoph Walker,* Alexi Crosby,[‡] Rachel J. Davies,[‡] Nicholas W. Morrell,[‡] and David C. Budd*

From the Respiratory Disease Area* and Global Discovery Chemistry,[†] Novartis Horsham Research Centre, Horsham; and the Department of Medicine,[‡] University of Cambridge School of Clinical Medicine, Addenbrooke's and Papworth Hospitals, Cambridge, United Kingdom

Mutations in the gene for the transforming growth factor (TGF)- β superfamily receptor, bone morphogenetic protein receptor II, underlie heritable forms of pulmonary arterial hypertension (PAH). Aberrant signaling via TGF- β receptor I/activin receptor-like kinase 5 may be important for both the development and progression of PAH. We investigated the therapeutic potential of a well-characterized and potent activin receptor-like kinase 5 inhibitor, SB525334 [6-(2-tert-butyl-5-[6-methyl-pyridin-2-yl]-1H-imidazol-4-yl)-quinoxaline] for the treatment of PAH. In this study, we demonstrate that pulmonary artery smooth muscle cells from patients with familial forms of idiopathic PAH exhibit heightened sensitivity to TGF- β 1 *in vitro*, which can be attenuated after the administration of SB525334. We further demonstrate that SB525334 significantly reverses pulmonary arterial pressure and inhibits right ventricular hypertrophy in a rat model of PAH. Immunohistochemical studies confirmed a significant reduction in pulmonary arteriole muscularization induced by monocrotaline

(used experimentally to induce PAH) after treatment of rats with SB525334. Collectively, these data are consistent with a role for the activin receptor-like kinase 5 in the progression of idiopathic PAH and imply that strategies to inhibit activin receptor-like kinase 5 signaling may have therapeutic benefit. (Am J Pathol 2009, 174:380–389; DOI: 10.2353/ajpath.2009.080565)

Pulmonary arterial hypertension (PAH) is a severe disease of the small pulmonary arteries characterized by vascular damage and narrowing of the vessels, leading to raised pulmonary artery pressure, right ventricular (RV) hypertrophy, and ultimately, right-sided heart failure and death. The combined effects of vasoconstriction, remodeling of the pulmonary vessel wall comprising abnormal endothelial and pulmonary artery smooth muscle cell (PASMC) proliferation and apoptosis, enhanced extracellular matrix deposition, and elevated thrombosis contribute to increased pulmonary vascular resistance and the resultant right-sided cardiac hypertrophy and mortality.¹ Although the exact molecular basis underlying the vascular damage remains unclear, genetic studies have linked germ-line mutations in a gene encoding the transforming growth factor β (TGF- β) superfamily receptor member *bone morphogenetic protein receptor 2* (BMPR-II) to the development of heritable forms of idiopathic pulmonary arterial hypertension (iPAH), encompassing familial and a proportion of sporadic cases of the disease.²

Supported in part by the Garfield Weston Trust (grant to N.W.M.).

Accepted for publication October 30, 2008.

Address reprint requests to David C. Budd, Respiratory Disease Area, Novartis Horsham Research Centre, Wimblehurst Rd., Horsham, West Sussex, RH12 5AB, UK. E-mail: david.budd@novartis.com.

Studies to assess the consequences of loss of BMPR-II have been undertaken to help elucidate the functional role of this receptor in the human pathology. Data from *in vitro* studies have shown that TGF- β addition to PSMCs isolated from patients with iPAH results in an elevated proliferative response compared with the effects mediated by addition of this growth factor to PSMCs from normotensive individuals.³ These data suggest that BMPR-II may repress the activity of the TGF- β /activin-like kinase 5 (ALK5) pathway in PSMCs from healthy individuals and that loss of BMPR-II may lead to unregulated TGF- β /ALK5 activity in PSMCs from patients with iPAH. Indeed, elevated Smad2 phosphorylation, a marker of TGF- β /ALK5 activity, can also be observed in endothelial cells isolated from plexiform lesions of patients with iPAH indicative of pathway activation.⁴ Furthermore, analysis of the expression levels of TGF- β 1, ALK5 and transforming growth factor- β receptor II (TGF- β RII) in leukocytes from patients with iPAH also reveals that the ratio of ALK5 expression to TGF- β RII is significantly higher in iPAH patients compared with normal controls, pointing toward an imbalance in expression patterns of components of the TGF- β pathway in circulating immune cells.⁵ Taken together, this evidence suggests that abnormal TGF- β /ALK5 signaling may be important in mediating the development and progression of iPAH.

Evidence has accumulated that highlights an important role for TGF- β signaling in the development and progression of certain pathophysiological features observed in preclinical models of experimental PAH. For instance, elevated expression levels of TGF- β ligands have been reported in the rat monocrotaline (MCT)⁶ and hypoxia models.⁷ In addition, altered expression of TGF- β ligands and type I receptors have been described in the pulmonary vasculature of a lamb model of congenital heart disease after aortopulmonary vascular graft.⁸ Studies addressing the functional role of TGF- β signaling in preclinical rodent models of PAH have recently been reported. Transgenic mice engineered to express an inducible kinase-deficient TGF- β RII receptor appear to be refractory to PAH induced by low oxygen suggesting that intact TGF- β is required for induction of PAH by hypoxia.⁹ Controversy exists to the role played by TGF- β signaling in MCT-mediated PAH in rats. A study by Zakrzewicz and colleagues¹⁰ demonstrated that components of the TGF- β signaling pathway are down-regulated in rats after MCT treatment, whereas a more recent study has shown elevated TGF- β pathway activation in pulmonary vascular cells of MCT-treated rats.¹¹ Interestingly, the latter study also demonstrated the ALK5 inhibitor, SD-208 prevented the development of MCT-induced PAH in rats. In contrast, delaying administration of SD-208 until established PAH had occurred resulted in a less pronounced impact on the ensuing pathologies, leading the authors to conclude that TGF- β /ALK5 signaling may play an important role in the initiation of experimental PAH, but a limited role in progression of established disease. These data would naturally imply that strategies to inhibit ALK5 signaling in iPAH may have limited therapeutic benefit because patients will usually present at later stages of the disease.

This study proposed to determine the validity of targeting the TGF- β pathway via a selective ALK5 inhibitor, SB525334. Here we demonstrate enhanced sensitivity to TGF- β in cells isolated from patients with familial iPAH, compared with normotensive controls, as shown by significantly higher expression levels of several TGF- β -regulated genes. We also show that abnormal TGF- β -mediated proliferation of PSMCs from patients with familial iPAH *in vitro* can be inhibited by the ALK5-selective compound, SB525334 with IC₅₀ values consistent with ALK5 inhibition. We have also tested the efficacy of SB525334 in reversing established PAH in the MCT rat model of disease. In contrast to the study using SD-208,¹¹ we demonstrate significant reversal of elevated mean pulmonary arterial pressure and inhibition of RV hypertrophy after MCT treatment using standard invasive readouts (right heart catheterization and Fulton index determination) or via noninvasive small animal echocardiography after oral administration of SB525334. Our computerized lung morphometry data suggest that small pulmonary artery remodeling induced after MCT insult is reversed by addition of SB525334 to rats and accounts for the significant improvement in hemodynamics after compound treatment. Our data support a role for ALK5 signaling in the latter stages of experimental PAH and implies that significant therapeutic benefit may be attained in the human pathology after systemic inhibition of the pathway.

Materials and Methods

Human PSMC Culture

PSMCs were isolated from the proximal pulmonary artery of patients with familial forms of iPAH ($n = 4$) and normotensive ($n = 3$) donor controls. These included two patients with a mutation in the kinase domain of BMPRII in which arginine or tyrosine is substituted for cysteine at position 347 (C347R and C347Y); a missense mutation in the cytoplasmic tail of BMPRII, leading to a serine in place of asparagine at position 903 (N903S); an exon 1 nonsense mutation at amino acid 9, W9X, predicted to lead to haploinsufficiency. Control PSMCs were obtained from patients undergoing lung resection for suspected malignancy.¹² The Papworth Hospital ethical review committee approved the study, and patients or relatives gave informed written consent. Cells were maintained in Dulbecco's modified Eagle's medium growth media containing 10% heat inactivated fetal calf serum and antibiotic-antimycotic and used between passages five and nine.

Reagents

Fibronectin, crotonine, PEG200, HCl, and NaOH were purchased from Sigma (Poole, UK). Human TGF- β 1 was purchased from R&D Systems (Abingdon, UK). Mouse anti- α -smooth muscle actin antibody was obtained from Sigma-Aldrich (Poole, Dorset, UK). Rabbit anti-von Willebrand factor (vWf) antibody, biotinylated swine anti-rabbit immunoglobulins, and biotinylated rabbit anti-mouse im-

munoglobulins, absorbed for rat immunoglobulins were purchased from (DAKO, Ely, UK). Rabbit anti-phospho Smad3 antibody was purchased from R&D Systems. The anti-phospho Smad2 antibody was purchased from Cell Signaling Technology (Hitchin, UK). The anti-BMPRII antibody was purchased from BD Transduction Laboratories (Oxford, UK). The echocardiographic system used was a Vivid 7 with pediatric sensor, analyzed on EchoPAC dimension software (GE Health Care, Bedford, UK). Millar catheters with Powerlab support were purchased from ADInstruments (Oxford, UK). SB525334 [6-(2-tert-butyl-5-[6-methyl-pyridin-2-yl]-1H-imidazol-4-yl)-quinoxaline], a well characterized and potent ALK5 inhibitor,¹³ was synthesized as described.¹⁴ All other reagents were from Sigma-Aldrich.

Proliferation Assays

Cell proliferation was assessed by bromodeoxyuridine (BrdU) incorporation. Briefly, PSMCs (1.2×10^3 per well) from donor controls or from a patient harboring an asparagine to serine mutation in BMPRII at position 903 were cultured on fibronectin (50 $\mu\text{g/ml}$)-coated 96-well plates in growth media. After 24 hours the media was replaced with serum-free media and cells incubated for a further 24 hours. Wells were then pre-incubated with 1 $\mu\text{mol/L}$ SB525334 or vehicle for 15 minutes before stimulating with 0.625 ng/ml of TGF- β 1. Proliferation was assessed after 6 days using a cell proliferation fluorescence kit (GE Health Care), according to the manufacturer's instructions. BrdU and Hoechst (Invitrogen, Paisley, UK) nuclear staining was assessed using the ImageXpress and MetaXpress software (Molecular Devices, Sunnyvale, CA).

Quantitative Reverse Transcriptase-Polymerase Chain Reaction (PCR) Analysis Using Patient Material

PSMCs from patients with familial iPAH ($n = 4$) and control donors ($n = 3$) were grown to confluence, serum-starved for 18 hours, and then stimulated with TGF- β 1 (2 ng/ml) for 0, 1, 4, and 12 hours. Total RNA was prepared using the Qiagen RNeasy mini kit according to the manufacturer's instructions, Qiagen, Crawley, UK. RNA was DNase-treated and 1 μg of total RNA reverse-transcribed using random hexamers and MMLV reverse transcriptase (Applied Biosystems, Warrington, UK). Real-time quantitative PCR was performed on GeneAmp 7900HT. Expression of target genes, *PAI-1*, *CCN1*, *CCN3*, and *JunB* were determined using assay-on-demand primer sets (Applied Biosystems). Reactions were performed using an Applied Biosystems ABI7900. All data were analyzed using ABI7900 SDS software (Applied Biosystems). Duplicate samples were run, transcripts were measured in picograms, and expression values were standardized to values obtained with control GAPDH (GAPDH Endogenous Control VIC/MGB Probe, Applied Biosystems). All data

are expressed as mean \pm SD and statistical analyses were performed using the Student's *t*-test.

Quantitative Reverse Transcriptase-PCR Analysis in Rat Lung Extract

Rat lungs were finely powdered in liquid nitrogen using mortar and pestle. Total RNA was prepared as outlined above. Expression of target genes, *CCN1* and *JunB* were determined using assay-on-demand primer sets (Applied Biosystems) as detailed above. All data are expressed as mean \pm SEM and statistical analyses were performed using the Student's *t*-test.

Western Blotting

Frozen rat lung tissue was homogenized in lysis buffer (250 mmol/L Tris-HCl, pH 6.8, 4% sodium dodecyl sulfate, 20% v/v/glycerol, and 1 Roche ethylenediaminetetraacetic acid-free protease inhibitor cocktail, Roche Burgess Hill, UK). Equal amounts of protein (70 μg) were resolved on a 12% reducing sodium dodecyl sulfate-polyacrylamide gel electrophoresis gels, transferred to a nitrocellulose membrane (Invitrogen). After blocking, the membranes were probed with anti-phospho-Smad3 (1:1000; Cell Signaling Technology, Inc.) overnight at 4°C. Blots were then incubated with an appropriate horseradish peroxidase-conjugated antibody and enhanced chemiluminescence reagent (Amersham Bioscience, Little Chalfont, UK). To confirm equal loading blots were incubated with an anti- α -tubulin antibody (Sigma).

MCT Rat Model of Pulmonary Hypertension

Animals were housed at 24°C in a 12-hour light-dark cycle. Food and water were accessible *ad libitum*. The studies reported here conformed to the UK Animals (scientific procedures) Act 1986. MCT-induced PAH was performed as previously described.¹⁵ Briefly, adult male Sprague-Dawley rats ($n = 10$ per group) were anesthetized and subcutaneously injected with 40 mg/kg of MCT or sterile saline. Before commencement of dosing at day 17 the extent of hypertensive pathology was determined in animals ($n = 5$) per group via echocardiography. A further group of animals was also assessed via surgery and catheterization. SB525334 compound was dosed orally (3 or 30 mg/kg) or vehicle alone was dosed daily until day 35, when the remaining animals were reassessed by echocardiography, surgery, and catheterization.

Surgical Assessment of PAH Pathologies

Systemic pressure was determined in anesthetized rats via tail cuff. The jugular vein was then surgically exposed and blood flow isolated with a distal ligature. A small hole was made in the vessel and a 2F Millar pressure/volume catheter introduced and progressed into the right ventricle, where an average RV pressure was measured during systole. After removal of catheter, animals were exsan-

guinated for pharmacokinetic profiling. The heart was then removed and the RV dissected from the LV and septum, and the weight ratio determined to provide Fulton index measurements. Lungs were excised from the rats and inflated with 10% neutral-buffered formalin and then immersed in neutral-buffered formalin to complete fixation for 24 to 48 hours. The left lobe was dissected and processed into paraffin wax using a Bayer VIP closed tissue processor, (Bayer Inc, Newbury, UK) and 3- μ m sections were cut, mounted, and dried before staining. Sections were stained for α -smooth muscle actin and von Willebrand factor (vWf) using a double-staining immunohistochemistry method (Ventana XT autoimmunostainer, Tuscon, AZ).

Echocardiographic Assessment

Echocardiographic assessments were performed by ultrasound on anesthetized animals. Briefly the pediatric probe was adjusted to ~400 images/second and placed in a parasternal long axis position to visualize the pulmonary artery outflow tract. Pulsed flow Doppler imaging was then overlaid to observe the dynamics of blood flow through the pulmonary artery valve. Changes in pulmonary artery acceleration time (time taken from start of flow to maximal velocity) and mid-systolic notch (degree of indent through deceleration flow) was determined. The probe was repositioned to view the RV wall and space at the level of valve movement. Motion mode analysis was then used to measure RV wall thickness during systole and diastole. Analysis was performed using EchoPAC dimension software, GE Healthcare, Bedford, UK. Results are expressed as mean \pm SEM. Statistical significance ($P < 0.01$) was determined using one-way analysis of variance and Kruskal-Wallis test.

Immunohistochemistry

For immunohistochemistry, tissue sections were treated in a 0.4 mol/L of sodium citrate buffer at pH 6.0 and antigen retrieval performed using a microwave (Surgipath, Peterborough, UK) followed by enzymatic digestion with Proteinase K (DakoCytomation, Ely, UK) for 10 minutes. Endogenous tissue peroxidase was quenched using hydrogen peroxidase blocking solution (DakoCytomation). Tissue Smad2 activity was assessed using an anti-phospho-Smad2 (1:600, Cell Signaling Technology) and an affinity-purified anti-rabbit streptavidin biotin complex (StreptABC) peroxidase technique (Vector Laboratories, Peterborough, UK). Antibody staining was visualized using 3-3'-diaminobenzidine hydrochloride substrate (DakoCytomation) and counterstained in Carrazzi's hematoxylin (Bios, Shelmersdale, UK).

Image Analysis

Slides were examined using a DMLB microscope, digital camera, and IM50 imaging software (Leica Microsystems, Milton Keynes, UK). Six ($\times 200$) random fields from each case were photographed and exported into a Q-Win digital image analysis package (Leica Microsystems)

and the total area of lung tissue (entire field minus alveolar spaces) quantified. Using the same high-power field, the program was repeated but with an additional step to include the lung tissue free from 3-3'-diaminobenzidine hydrochloride or Sirius Red stain. The area of phospho-Smad2-positive stained tissue was then expressed as a percentage of the total parenchymal area.

Results

Familial iPAH PSMCs Exhibit Heightened Sensitivity to TGF- β 1

Abnormal proliferation of PSMCs isolated from patients with iPAH in response to TGF- β 1 addition *in vitro* has

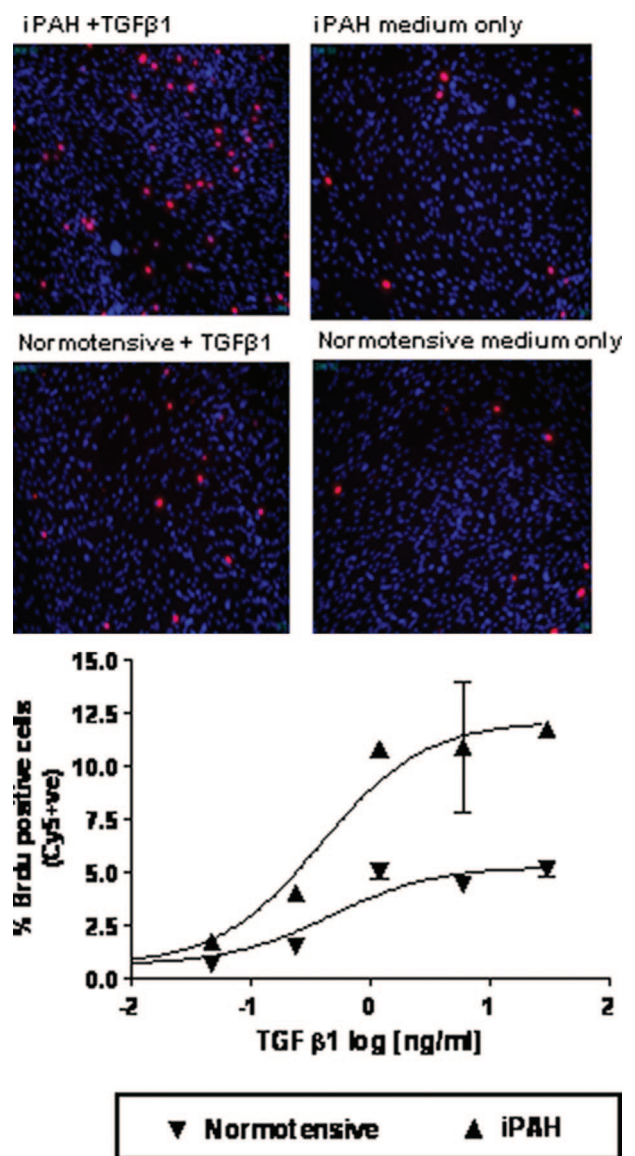


Figure 1. PSMCs derived from iPAH or normotensive patients were plated at equal cell densities in 96-well plates. Cells were serum-starved for 48 hours before treatment with 0.625 ng/ml of TGF- β 1. Proliferation was measured by BrdU incorporation after 6 days. The percent of positive cells was calculated as the number of BrdU-positive cells/total number of cells determined by Hoechst staining. Original magnifications, $\times 100$.

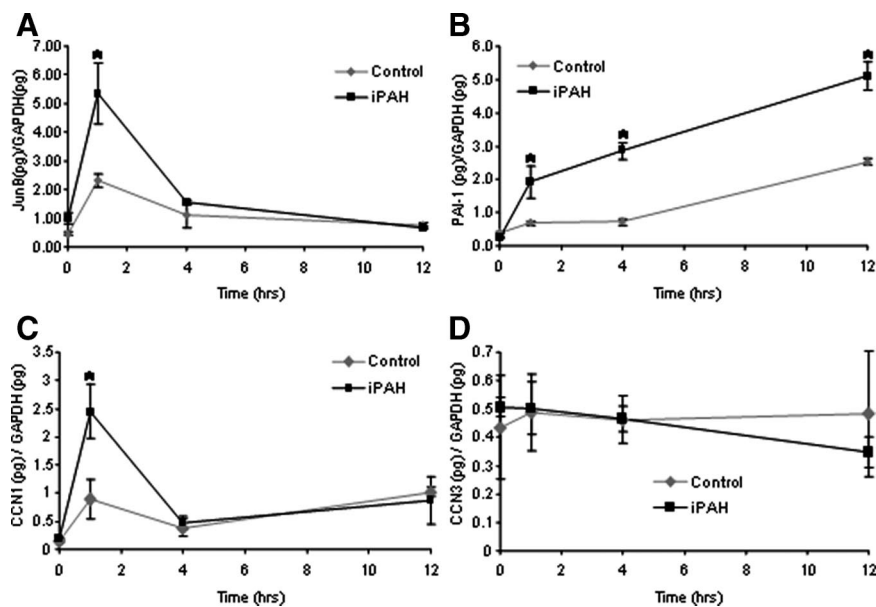


Figure 2. Enhanced transcriptional responses to TGF- β 1 on iPAH PASMCS. iPAH and control PASMCS were cultured to confluence, serum-starved, and treated for 0, 1, 4, and 12 hours in the presence or absence of TGF- β 1 (2 ng/ml). Cells were cultured from four individuals with iPAH and three control individuals. Total RNA was harvested, reverse-transcribed into cDNA, and subjected to real-time PCR analysis performed in duplicate with primers recognizing *JunB* (A), *PAI-1* (B), *CCN1* (C), and *CCN3* (D). Ratios of target genes/GAPDH RNA levels \pm SD plotted. * $P < 0.05$ (Student's *t*-test) compared with respective control time point.

been described and proposed to potentially underlie the pathological muscularization of small pulmonary arterioles characteristically observed in the pulmonary vasculature of affected individuals.³ We have recapitulated these findings by demonstrating elevated concentration-dependent TGF- β 1-mediated proliferation of PASMCS isolated from a familial iPAH patient with defined BMPR-II mutation compared with a normotensive donor control using BrdU incorporation to visualize active DNA synthesis (Figure 1). The potency of TGF- β 1 to mediate BrdU incorporation in PASMCS from affected and nonaffected donors did not differ (EC_{50} of 394 pg/ml and 470 pg/ml for familial iPAH and normotensive, respectively). The temporal regulation of expression of the classical TGF- β responsive genes, *PAI-1*, *JunB*, and two members of the CCN family, *CCN1* (*Cyr61*) and *CCN3* (*Nov*), were investigated after TGF- β 1 stimulation. In keeping with previous studies investigating the effects of TGF- β 1 on lung fibroblasts,¹⁶ TGF- β 1 induced transcriptional activation of *JunB*, *PAI-1*, and *CCN1* but not *CCN3* in a time-dependent manner (Figure 2, A–D). Consistent with the enhanced proliferative effects of TGF- β 1 (Figure 2), familial iPAH PASMCS exhibited a significantly enhanced transcriptional response to TGF- β 1 as determined by *JunB*, *PAI-1*, and *CCN1* expression levels (Figure 2, A–C). Collectively these data support the notion that multiple aspects of TGF- β 1 signaling are enhanced in PASMCS from familial iPAH patients after pathway activation.

Enhanced Proliferation of hPAH PASMCS in Response to TGF- β 1 Is Mediated via ALK5

We have used the recently reported potent and selective ALK5 kinase inhibitor, SB525334¹³ to assess the contribution of ALK5 in mediating the abnormal TGF- β 1 responses observed in familial iPAH PASMCS. Significantly, the TGF- β 1-mediated proliferation of familial iPAH PASMCS is abolished by pre-incubation of cells with a

potent ALK5 kinase inhibitor, SB525334 implying that ALK5 transduces the abnormal pro-proliferative signal after ligand addition to these cells *in vitro* (Figure 3). Consistent with previously published data,¹³ SB525334 inhibited TGF- β 1-mediated proliferation of familial iPAH PASMCS at an IC_{50} of 295 nmol/L (data not shown). Collectively, our *in vitro* data imply that PASMCS isolated from familial iPAH patients exhibit increased sensitivity to TGF- β 1 addition compared with PASMCS isolated from normotensive controls. Further, this differential sensitivity to exogenously applied growth factor results in elevated proliferation that appears to be mediated by ALK5.

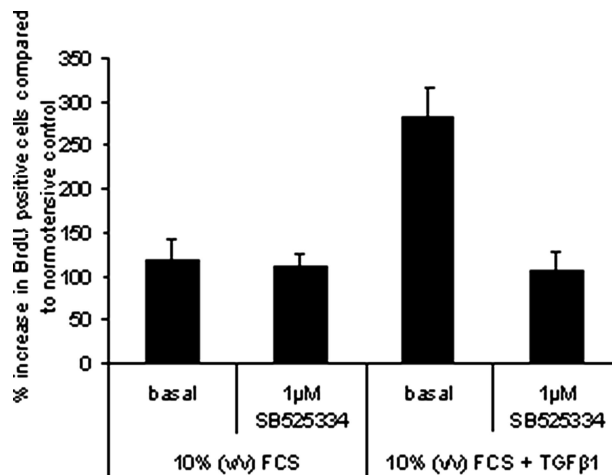


Figure 3. PASMCS derived from iPAH patients were plated at equal cell densities in 96-well plates. Cells were starved for 48 hours before treatment with 0.625 ng/ml of TGF- β 1 in growth media containing 10% (v/v) fetal calf serum. One μ mol/L of SB525334 was added 15 minutes before the addition of TGF- β 1. Proliferation was measured by BrdU incorporation after 6 days. The percentage of cells that were BrdU-positive was calculated and normalized to the average BrdU incorporation in untreated normotensive cells.

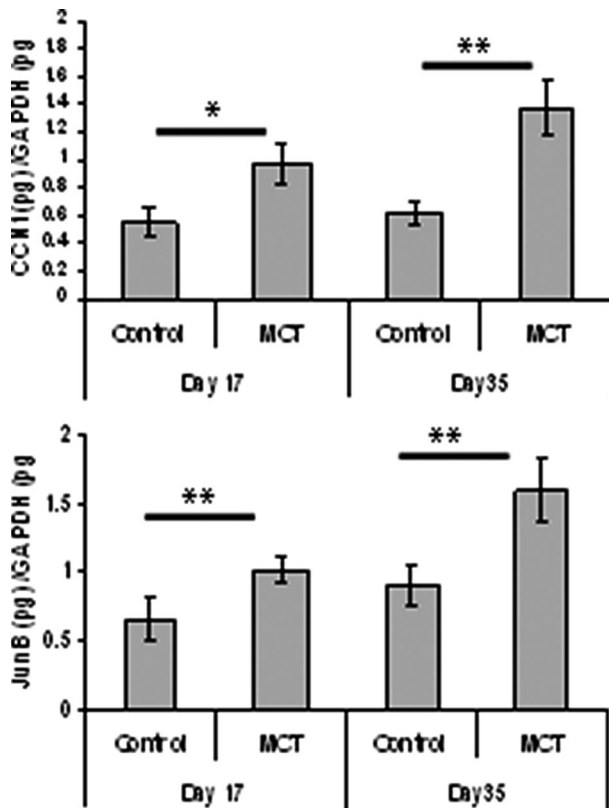


Figure 4. MCT-treated rat lungs exhibit enhanced transcription of TGF- β -regulated genes. Total RNA from rat lungs were harvested 17 days after MCT treatment ($n = 10$) or vehicle alone ($n = 5$) and 35 days after MCT treatment ($n = 10$) or vehicle alone ($n = 5$). The expression of *JunB* and *CCN1* was determined by real-time PCR analysis. *CCN1* (top) and *JunB* (bottom) expression were determined and the ratios of target genes/GAPDH RNA levels \pm SEM plotted. * $P < 0.05$, ** $P < 0.01$ (Student's *t*-test) compared with respective control time point.

MCT-Induced Rises in RV Pressure and Hypertrophy Are Stabilized by ALK5 Inhibition

A rat MCT model of pulmonary hypertension was used to determine the effects of therapeutic ALK5 inhibition using SB525334 on the development and progression of PAH pathologies *in vivo*. Previously published work has led to some controversy about the role played by TGF- β signaling in MCT-mediated iPAH in rats. A study by Zakrzewicz and colleagues¹⁰ demonstrated that components of the TGF- β signaling pathway are down-regulated in rats after MCT treatment, whereas a more recent study has shown elevated TGF- β pathway activation in pulmonary vascular cells of MCT-treated rats.¹¹ We have observed that the classically TGF- β -regulated genes, *CCN1* and *JunB*, are significantly elevated in whole rat lung tissue after MCT treatment at day 17 and day 35 compared with vehicle-treated animals (Figure 4). In addition, we have observed an elevation in phosphorylation of Smad2 (Figure 5, D and E) and Smad3 (Figure 5, A and C) in whole lung tissue after administration of MCT. Taken together, these data are consistent with the notion that activation of the TGF- β /ALK5 pathway occurs in this experimental model of pulmonary hypertension. Interestingly, the levels of BMPR-II in rat lung are markedly diminished throughout

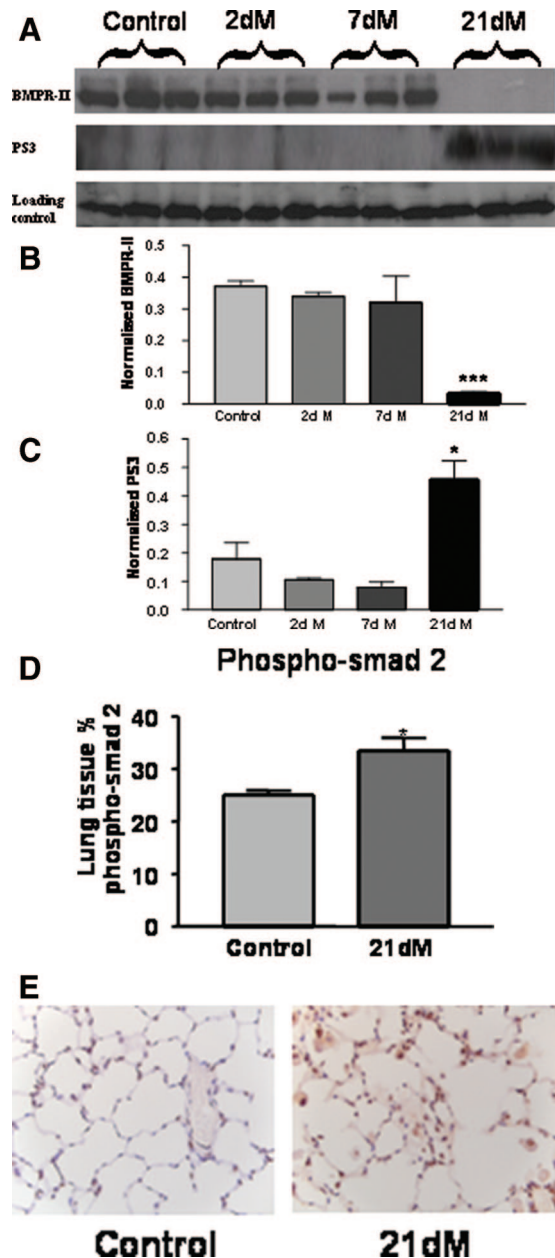


Figure 5. A: Changes in the expression of bone morphogenetic protein (BMPR-II) and phosphorylated Smad 3 (PS3) in the lungs of MCT-treated rats was assessed by immunoblotting (dM indicates days of MCT treatment). B and C: Quantification of immunoblotting for BMPR-II (B) and PS3 (C). The data shown are the mean density of the appropriate band \pm SEM. * $P < 0.05$, *** $P < 0.001$ (Student's *t*-test) compared with the respective control time point. D: Quantification of the expression of phosphorylated Smad 2 in the lung by immunohistochemistry. The data plotted are the mean area \pm SEM of positive stained tissue expressed as a percentage of the total parenchymal area. * $P < 0.05$ (Student's *t*-test) compared with control lung tissue area. E: Representative pictures of immunohistochemistry in lung tissue for phospho-Smad 2, brown indicates phospho-Smad 2 expression. Original magnifications, $\times 40$.

the same time period after MCT administration (Figure 5, A and B) perhaps pointing toward an interaction between these pathways.

Previous optimization studies in rats had provided a model, which, after subcutaneous injection of MCT, established hypertensive pathologies by day 17, which became progressively worse, peaking at days 28 to 35

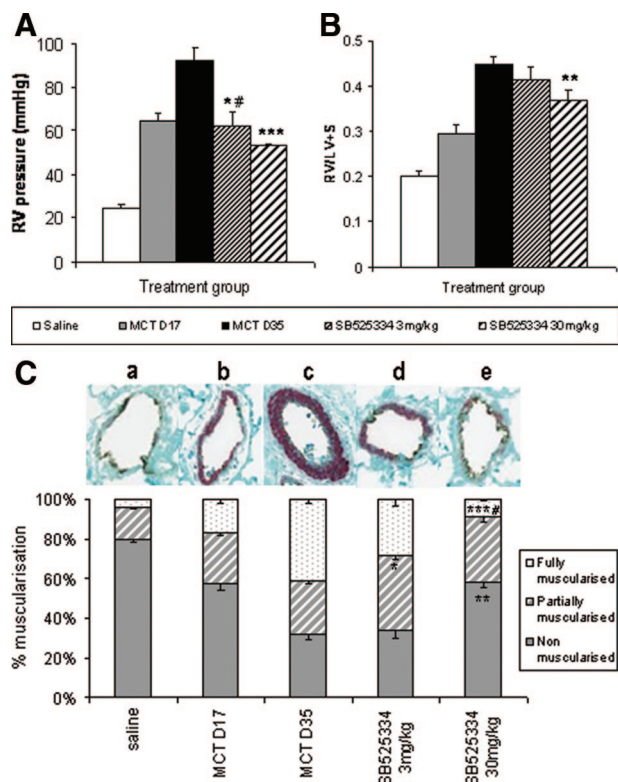


Figure 6. RV systolic pressure levels (A) and Fulton index measures (RV/LV + S weight ratio) (B) in rats exposed to MCT or saline-negative control. Analysis was performed in rats at the point of established PAH pathology (day 17, gray bars), after which animals were orally treated with either vehicle (black bars), 3 mg/kg (fine hatched bars), or 30 mg/kg (thick hatched bars) SB525334 until day 35. Values are means \pm SEM. C: Arteriole remodeling in rats after MCT exposure. Inflated lung sections ($n = 10$ per group) were stained with vWf and anti- α -smooth muscle actin, and then 200 small vessels ($<100 \mu\text{mol/L}$) per section were analyzed by an investigator unaware of the source of tissue. Each vessel was assigned as either nonmuscularized (no α -smooth muscle actin staining), partially muscularized, or fully muscularized (thick unbroken wall of smooth muscle), and then the percentage distribution of each calculated per group. A representative picture of the predominantly altered vessel phenotype is provided above each group (a–e). Values are the means \pm SEM, * $P < 0.05$ for MCT day 17 versus vehicle-treated control, * $P < 0.01$, ** $P < 0.001$, *** $P < 0.001$ for rct day 35 versus vehicle-treated control (Student's *t*-test).

(data not shown). RV pressure rose from 25 to 64 mmHg by day 17, at which point ALK5 was inhibited via oral dosing of SB525334. Vehicle-treated animals continued to worsen, with a mean RV pressure of 92 mmHg attained by day 35. This deterioration was abrogated by treatment with 3 mg/kg of SB525334 (62 mmHg), with a trend toward reversal observed in 30 mg/kg treated animals (53 mmHg) (Figure 6A). The progression of RV hypertrophy measured by the Fulton index (RV/LV + S) was more pronounced beyond day 17. Treatment of animals with SB525334 significantly inhibited RV hypertrophy as the Fulton index ratio was reduced from 0.45 in vehicle-treated animals compared with 0.37 in 30 mg/kg SB525334-treated animals (Figure 6B).

ALK5 Inhibition Reverses Pulmonary Arteriole Muscularization

The majority (80%) of small vessels ($<100 \mu\text{mol/L}$) in the lung are nonmuscularized, as shown in saline-exposed

animals and the associated picture (Figure 6Ca), the remainder of which show partial (16%) or full (4%) muscularization. At day 17 after MCT exposure, nonmuscularized vessels were reduced to 56%, whereas partially muscularized vessels had risen to 26% and fully muscularized vessels to 17% (a representative shown in Figure 6Cb). Staining for α -smooth muscle actin continued to worsen by day 35, with fully muscularized vessels (a representative shown in Figure 6Cc) now forming the majority of those counted (41%) and representing a 10-fold increase over normal animals. Treatment with 3 mg/kg of SB525334 reduced the proportion of fully muscularized vessels to 28%, which was primarily absorbed by a partially muscularized phenotype (Figure 6Cd). However, 30 mg/kg treatment returned fully muscularized vessel distribution beyond that seen at day 17 and approaching the phenotype observed in saline-exposed controls (Figure 6Ce).

Echocardiographic Analysis Demonstrates Inter- and Intra-Animal Stabilization and Reversal of Pathologies by ALK5 Inhibition

An echocardiographic pulsed Doppler profile (velocity/time) of blood flow through the pulmonary valve was used as a serial, noninvasive measure of hypertensive rises in RV pressure. Normal animals with pulmonary pressures in the region of 25 mmHg show characteristic symmetry during a gradual rise and fall of flow through the pulmonary valve (Figure 7, A, D, and G). In the 17 days after MCT exposure, such profiles change as pressure rises (~ 60 mmHg), resulting in a more acute, and therefore shorter, rise to maximum velocity (V_{max}), apparent as a decreased pulmonary artery acceleration time. Furthermore, the first signs of mid-systolic notch appear (Figure 7, B, E, and H). By day 35, vehicle-treated animals show an abrupt spike toward V_{max} , followed by a pronounced notch in the decelerating flow in keeping with the further rise in pressure (~ 90 mmHg) (Figure 7, B and C). However, after treatment with 3 mg/kg of SB525334, the flow profile has apparently stabilized in the representative animal shown (Figure 7, E and F), and reversed to a normotensive-like profile in animals given a 30 mg/kg dose, also shown in scans of a representative animal (Figure 7, H and I).

Quantification of the changes observed by echocardiographic analysis is shown in Figure 8. RV wall thickness was assessed during both diastole and systole and showed a subtle increase in all MCT-exposed groups from day 0 to 17, reaching 0.9- to 1-mm and 1- to 1.3-mm measurements, respectively. By day 35, however, wall measurements had profoundly risen in vehicle-treated animals up to 1.6 mm in diastole and 2.3 mm during systole. A trend toward decreasing these measures of RV hypertrophy was observed in SB525334-treated groups, although true statistically significant attenuation was only achieved in 30 mg/kg animals measured during systole—a decrease from 2.3 to 1.8 mm (Figure 8, A and B). The decrease in PA acceleration time is shown as a steady decline from day 0 normotensive animals at 40

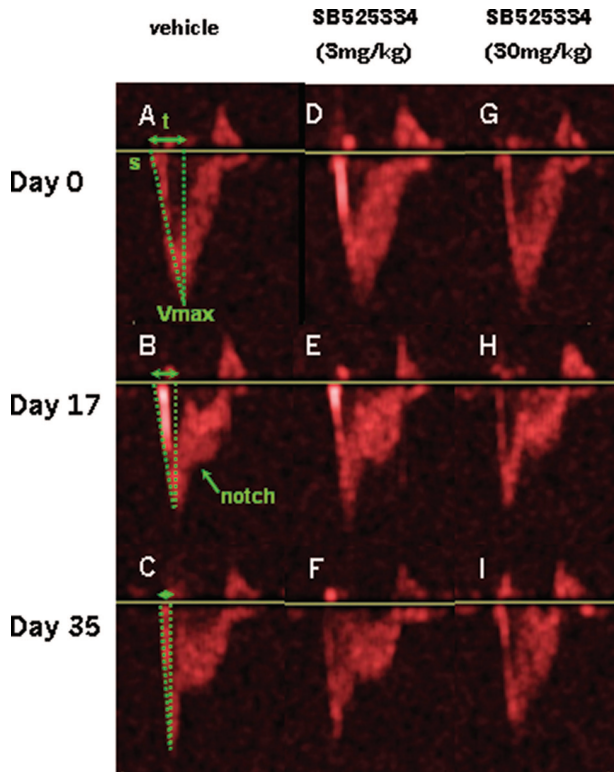


Figure 7. Pulsed wave Doppler profiles of blood flow through the pulmonary artery outflow tract. The start of flow (s) reaches a maximum velocity (V_{max}) within a given time (t), known as the pulmonary artery acceleration time, which increases in accordance with pulmonary artery pressure (A–C). The smooth flow deceleration of a normal RV circulation can also change with hypertension to show a characteristic mid-systolic notch (B). Day 0 profiles (A, D, and G) are of normal animals (Veh), whose hypertensive state is seen at day 17 after MCT exposure, and immediately before commencement of compound dosing (B, E, and H). The resultant stabilization, or reversal of hypertensive pathologies, is shown at day 35 (C, F, and I) in the same animals shown at day 17.

ms, to 27 ms at days 17 and 19 by day 35. Minimal impact is observed in animals dosed at 3 mg/kg of SB525334, whereas the 30 mg/kg dose stabilized pathology at 28 ms (Figure 8C). The severity of mid-systolic notch was quantified by applying a score between 0 and 3 to each wave profile observed for each animal (Figure 8D). Saline-exposed normotensive animals display a smooth deceleration profile and tend to score 0 or 1 (eg, Figure 7A). Mildly hypertensive animals with pressures between 40 and 60 mmHg show a clear notch and score 1 to 2 (eg, Figure 7B) and profoundly hypertensive individuals with pressures >60 mmHg tend to score 2 to 3 (eg, Figure 7C). Mean scores show a steady and uniform rise from 0 to 1.4 to 2.9 in MCT-exposed, vehicle-treated animals from day 0 to 17 to 35, respectively. A trend toward attenuation is observed in 3 mg/kg SB525334-treated animals, although 30 mg/kg dosing was required to significantly reverse the presence of notch to 0.8 —below that seen at day 17 in all MCT-exposed groups (Figure 8D).

Discussion

The data described in this study lend support to the notion that aberrant TGF- β 1/ALK5 signaling may underlie

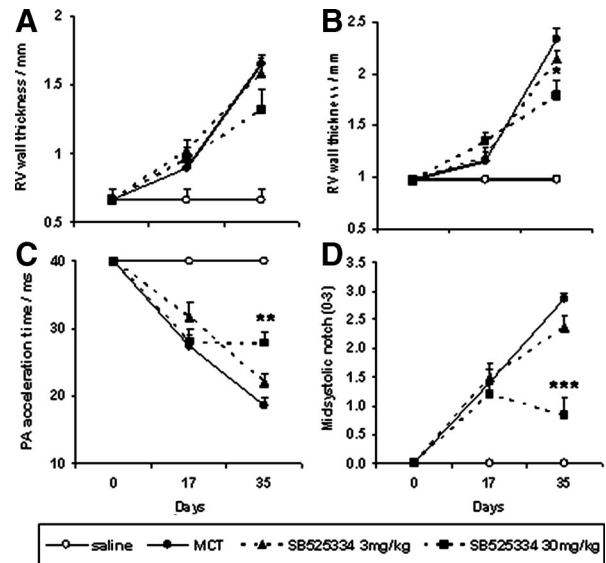


Figure 8. Echocardiographic measurement of pulmonary hypertensive parameters in animals serially investigated after MCT exposure at day 0, the establishment of reliable pathologies at day 17, and the dosing of either vehicle, or SB525334 from days 17 to 35 (noted above). RV wall thickness during systole (A) and diastole (B), pulmonary artery acceleration time (C) and degree of mid-systolic notch (D) are shown. Vehicle versus MCT-exposed; vehicle-treated groups are represented by open and closed circles, respectively. Treated groups are shown by dashed lines at 3 mg/kg (closed triangle) and 30 mg/kg (closed square). Values are means \pm SEM. * P < 0.01 versus day 35 vehicle-treated control (one-way analysis of variance and Kruskal-Wallis test).

the pulmonary vascular remodeling and the elevated vascular resistance and subsequent RV cardiac hypertrophy after MCT treatment in rats. Analysis of the lung morphometric data representative of the muscularization of the small to medium-sized pulmonary arterioles of MCT-treated animals suggests that application of SB525334 results in reverse remodeling of these resistance vessels. These data imply that one of the functions of the TGF- β /ALK5 pathway in this preclinical model of PAH is to participate in the remodeling of the pulmonary vascular wall in response to injury. Indeed, aberrant TGF- β pathway signaling has been implicated in mediating remodeling events in other injury-induced models of vascular disease.^{17–19}

Abnormal TGF- β 1/ALK5 signaling has been implicated in a number of preclinical models of PAH including aortopulmonary shunt model in lambs,⁸ hypoxia-induced PAH⁹ in mouse, and most recently the MCT model in rats.^{10,11} Some controversy has emerged in the field with regard to modulation of the TGF- β pathway in the rat MCT model. Zakrzewicz and colleagues¹⁰ observed an extensive reduction in components of the ALK5/Smad pathway after MCT insult in rats and suggested that the pathway may be significantly blunted under these experimental conditions. In contrast, Zaiman and colleagues¹¹ have suggested that Smad-dependent signaling mediated by ALK5 after MCT treatment may be elevated in the pulmonary vasculature of rats and have demonstrated prevention of the induction of PAH in these animals when treated prophylactically with an orally bio-available ALK5 inhibitor. Our own data are consistent with an elevation of TGF- β /ALK5 signaling after MCT administration in rats.

A review of the available data from external publications and our own data suggests that aberrant TGF- β /ALK5 signaling observed in the preclinical models of iPAH translate into the human pathology. Previous functional studies in PASMCs isolated from patients presenting with iPAH suggest that loss of growth suppression by the BMP pathway and a gain of proliferation via TGF- β 1 could contribute to the enhanced growth of these cells in the injured pulmonary vascular wall.³ Activation of the TGF- β /ALK5/Smad signaling pathway has also been observed in pulmonary vascular cells of remodeled pulmonary arteries of patients with iPAH assessed via immunohistochemistry.⁴ We have now presented evidence for increased sensitivity of PASMCs from familial iPAH patients with defined BMPR-II mutations in response to exogenously applied TGF- β 1 as shown by elevated TGF- β 1-driven transcription of *PAI-1*, *JunB*, and *CCN1* and enhanced growth factor-mediated proliferation. Collectively, these data imply that dysfunctional TGF- β /ALK5 signaling may underlie the abnormal vascular remodeling characteristically observed in the pulmonary vasculature of individuals with familial iPAH because of loss of BMPR-II function.

The pleiotropic and context-dependent nature of the signals that are transduced after ALK5 activation suggests that numerous mechanisms may underlie the dysfunctional signaling that contribute to initiation and progression of familial iPAH. Up-regulation of TGF- β 1 after arterial injury results in the activation of various downstream pathways that stimulate the proliferation and migration of vascular smooth muscle cells, as well as the production of local extracellular matrix proteins. The loss of BMPR-II function via germ-line mutations and an inability to promote PASMC apoptosis²⁰ combined with elevated TGF- β 1/ALK5-mediated proliferation of this cell population, may favor the muscularization and subsequent remodeling of the small pulmonary arterioles after lung injury. TGF- β 1 signaling may also indirectly promote vascular remodeling by inducing the expression of other potent vascular mitogens such as ET-1.^{21,22} Elevated TGF- β 1/ALK5 in PASMCs may also participate in the promotion of microthrombotic events in the pulmonary vasculature by regulating the expression and release of PAI-1 from PASMCs.^{23,24}

The data described by Zaiman and colleagues¹¹ support a role for ALK5 signaling in the early pathological processes during the induction of PAH after MCT challenge in rats but questions the therapeutic relevance of targeting this pathway for treating established disease. In our own studies we have administered SB525334 prophylactically to rats in the MCT model and have observed significant prevention of MCT-induced PAH pathologies (unpublished observations), confirming that the ALK5 pathway is indeed involved in the induction phase of MCT-induced PAH in rats. Our interpretation of the data presented here is that ALK5 plays a significant pathophysiological role in the progression of established disease in the rat MCT model and furthermore, inhibition of the pathway may provide a novel therapeutic option for treating familial iPAH. The data we have presented are consistent with a role for ALK5 in mediating remodeling of

the small- and medium-sized pulmonary arterioles perhaps via enhanced proliferation of PASMCs surrounding the pulmonary arterial wall.

The enhanced efficacy of SB525334 described here compared with the moderate efficacy of SD-208 presented by Zaiman and colleagues¹¹ in inhibiting the MCT-induced PAH pathologies, may be because of differences in pharmacokinetics of each ALK5 inhibitor or alternatively to the number of days of treatment with the kinase inhibitors (9 days for SD208 and 17 days for SB525334). It may also be possible that monitoring an individual animal with noninvasive, clinically relevant echocardiographic readouts, before and after therapy, may provide a clearer view of the impact of ALK5 inhibition.

Loss of BMPR-II function after germ-line mutation has been strongly linked to the development and progression of familial and sporadic forms of iPAH.^{2,25} We and others have demonstrated that vascular smooth muscle cells isolated from patients with familial and sporadic iPAH exhibit elevated ALK5 signaling.³ Taken together these findings imply that ALK5 signaling is controlled by the BMPR-II pathway in pulmonary vascular smooth muscle cells via mechanisms that have not been fully elucidated. Indeed, a recent study has shown that patients exhibiting a combination of heterozygous BMPR-II mutations and activating polymorphisms in the TGF- β 1 gene are diagnosed earlier with familial iPAH and genetic penetrance is enhanced.²⁶ Thus, understanding the molecular mechanisms that lead to elevated ALK5 signaling as a result of loss of functional BMPR-II may be key in understanding the pathophysiological role for TGF- β /ALK5 signaling in familial and sporadic iPAH.

References

1. Chan SY, Loscalzo JJ: Pathogenic mechanisms of pulmonary arterial hypertension. *J Mol Cell Cardiol* 2008, 44:14–30
2. Lane KB, Machado RD, Pauculo MW, Thomson JR, Phillips III JA, Loyd JE, Nichols WC, Trembath RC: Heterozygous germline mutations in BMPR2, encoding a TGF-beta receptor, cause familial primary pulmonary hypertension. The International PPH Consortium. *Nat Genet* 2000, 26:81–84
3. Morrell NW, Yang X, Upton PD, Jourdan KB, Morgan N, Sheares KK, Trembath RC: Altered growth responses of pulmonary artery smooth muscle cells from patients with primary pulmonary hypertension to transforming growth factor-beta(1) and bone morphogenetic proteins. *Circulation* 2001, 104:790–795
4. Richter A, Yeager ME, Zaiman A, Cool CD, Voelkel NF, Tuder RM: Impaired transforming growth factor-beta signalling in idiopathic pulmonary arterial hypertension. *Am J Respir Crit Care Med* 2004, 170:1340–1348
5. Jachec W, Foremny A, Domal-Kwiatkowska D, Smolik S, Tomasik A, Mazurek U, Wodniecki J: Expression of TGF-beta1 and its receptor genes (TbetaR I, TbetaR II, and TbetaR III-beta glycan) in peripheral blood leucocytes in patients with idiopathic pulmonary arterial hypertension and Eisenmenger's syndrome. *Int J Mol Med* 2008, 21: 99–107
6. Arcot SS, Lipke DW, Gillespie MN, Olson JW: Alterations of growth factor transcripts in rat lungs during development of monocrotaline-induced pulmonary hypertension. *Biochem Pharmacol* 1993, 46: 1086–1091
7. Jiang Y, Dai A, Li Q, Hu R: Hypoxia induces transforming growth factor-beta1 gene expression in the pulmonary artery of rats via

- hypoxia-inducible factor-1 α . *Acta Biochim Biophys Sin (Shanghai)* 2007, 39:73–80
8. Mata-Greenwood E, Meyrick B, Steinhorn RH, Fineman JR, Black SM: Alterations in TGF- β 1 expression in lambs with increased pulmonary blood flow and pulmonary hypertension. *Am J Physiol* 2003, 285:L209–L221
 9. Chen YF, Feng JA, Li P, Xing D, Zhang Y, Serra R, Ambalavanan N, Majid-Hassan E, Oparil S: Dominant negative mutation of the TGF- β 1 receptor blocks hypoxia-induced pulmonary vascular remodeling. *J Appl Physiol* 2006, 100:564–571
 10. Zakrzewicz A, Kouri FM, Nejman B, Kwapiszewska G, Hecker M, Sandu R, Dony E, Seeger W, Schermuly RT, Eickelberg O, Morty RE: The transforming growth factor- β /Smad2,3 signalling axis is impaired in experimental pulmonary hypertension. *Eur Respir J* 2007, 29:1094–1104
 11. Zaiman AL, Podowski M, Medicherla S, Gordy K, Xu F, Zhen L, Shimoda LA, Neptune E, Higgins L, Murphy A, Chakravarty S, Protter A, Sehgal PB, Champion HC, Tudor RM: Role of TGF- β /ALK5 kinase in monocrotaline-induced pulmonary hypertension. *Am J Respir Crit Care Med* 2008, 177:896–905
 12. Yang J, Davies RJ, Southwood M, Long L, Yang X, Sobolewski A, Upton PD, Trembath RC, Morrell NW: Mutations in bone morphogenetic protein type II receptor cause dysregulation of Id gene expression in pulmonary artery smooth muscle cells: implications for familial pulmonary arterial hypertension. *Circ Res* 2008, 102:1212–1221
 13. Grygielko ET, Martin WM, Tweed C, Thornton P, Harling J, Brooks DP, Laping NJ: Inhibition of gene markers of fibrosis with a novel inhibitor of transforming growth factor- β type I receptor kinase in puromycin-induced nephritis. *J Pharmacol Exp Ther* 2005, 313:943–951
 14. Gaster LM, Hadley MS, Harling JD, Harrington FP, Heer JP, Heightman TD: PCT Int. Appl. 2001, WO2001062756A1. *Chem Abstr* 2001, 135:195566
 15. Dumitrascu R, Weissmann N, Ghofrani HA, Dony E, Beuerlein K, Schmidt H, Stasch JP, Gnoth MJ, Seeger W, Grimminger F, Schermuly RT: Activation of soluble guanylate cyclase reverses experimental pulmonary hypertension and vascular remodeling. *Circulation* 2006, 113:286–295
 16. Renzoni EA, Abraham DJ, Howat S, Shi-Wen X, Sestini P, Bou-Gharios G, Wells AU, Veeraraghavan S, Nicholson AG, Denton CP, Leask A, Pearson JD, Black CM, Welsh KI, du Bois RM: Gene expression profiling reveals novel TGF β targets in adult lung fibroblasts. *Respir Res* 2004, 5:24
 17. Fu K, Corbley MJ, Sun L, Friedman JE, Shan F, Papadatos JL, Costa D, Lutterodt F, Sweigard H, Bowes S, Choi M, Boriack-Sjodin PA, Arduini RM, Sun D, Newman MN, Zhang X, Mead JN, Chuaqui CE, Cheung HK, Zhang X, Cornebise M, Carter MB, Josiah S, Singh J, Lee WC, Gill A, Ling LE: SM16, an orally active TGF β type I receptor inhibitor prevents myofibroblast induction and vascular fibrosis in the rat carotid injury model. *Arterioscler Thromb Vasc Biol* 2008, 28:665–671
 18. Khan R, Agrotis A, Bobik A: Understanding the role of transforming growth factor- β 1 in intimal thickening after vascular injury. *Cardiovasc Res* 2007, 74:223–234
 19. Ikeda Y, Imai Y, Kumagai H, Nosaka T, Morikawa Y, Hisaoka T, Manabe I, Maemura K, Nakaoka T, Imamura T, Miyazono K, Komuro I, Nagai R, Kitamura T: Vasorin, a transforming growth factor β -binding protein expressed in vascular smooth muscle cells, modulates the arterial response to injury in vivo. *Proc Natl Acad Sci USA* 2004, 101:10732–10737
 20. Zhang S, Fantozzi I, Tigno DD, Yi ES, Platoshyn O, Thistlethwaite PA, Kriett JM, Yung G, Rubin LJ, Yuan JX: Bone morphogenetic proteins induce apoptosis in human pulmonary vascular smooth muscle cells. *Am J Physiol* 2003, 285:L740–L754
 21. Shi-Wen X, Rodríguez-Pascual F, Lamas S, Holmes A, Howat S, Pearson JD, Dashwood MR, du Bois RM, Denton CP, Black CM, Abraham DJ, Leask A: Constitutive ALK5-independent c-Jun N-terminal kinase activation contributes to endothelin-1 overexpression in pulmonary fibrosis: evidence of an autocrine endothelin loop operating through the endothelin A and B receptors. *Mol Cell Biol* 2006, 26:5518–5527
 22. Castañares C, Redondo-Horcajo M, Magán-Marchal N, ten Dijke P, Lamas S, Rodríguez-Pascual F: Signalling by ALK5 mediates TGF- β -induced ET-1 expression in endothelial cells: a role for migration and proliferation. *J Cell Sci* 2007, 120:1256–1266
 23. Ikeda H, Tamaki K, Ueda S, Kato S, Fujii M, Ten Dijke P, Okuda S: Smad protein and TGF- β signalling in vascular smooth muscle cells. *Int J Mol Med* 2003, 11:645–650
 24. Samarakoon R, Higgins CE, Higgins SP, Kutz SM, Higgins PJ: Plasminogen activator inhibitor type-1 gene expression and induced migration in TGF- β 1-stimulated smooth muscle cells is pp60(c-src)/MEK-dependent. *J Cell Physiol* 2005, 204:236–246
 25. Thomson JR, Machado RD, Pauciulo MW, Morgan NV, Humbert M, Elliott GC, Ward K, Yacoub M, Mikhail G, Rogers P, Newman J, Wheeler L, Higenbottam T, Gibbs JS, Egan J, Crozier A, Peacock A, Allcock R, Corris P, Loyd JE, Trembath RC, Nichols WC: Sporadic primary pulmonary hypertension is associated with germline mutations of the gene encoding BMPR-II, a receptor member of the TGF- β family. *J Med Genet* 2000, 37:741–745
 26. Phillips III JA, Poling JS, Phillips CA, Stanton KC, Austin ED, Cogan JD, Wheeler L, Yu C, Newman JH, Dietz HC, Loyd JE: Synergistic heterozygosity for TGF β 1 SNPs and BMPR2 mutations modulates the age at diagnosis and penetrance of familial pulmonary arterial hypertension. *Genet Med* 2008, 10:359–365